Kinetic Analysis of Calcein and Calcein−Acetoxymethylester Efflux Mediated by the Multidrug Resistance Protein and P-Glycoprotein

M. Essodaïgui,[‡] H. J. Broxterman,[§] and A. Garnier-Suillerot*,[‡]

Laboratoire de Physicochimie Biomoléculaire et Cellulaire (URA CNRS 2056), Université Paris Nord, Bobigny 93017, France, and Department of Medical Oncology, Academisch Ziekenhuis Vrije Universiteit, de Boelelaan 1117, 1081 HV Amsterdam, The Netherlands

Received July 24, 1997; Revised Manuscript Received November 10, 1997

ABSTRACT: Multidrug resistance protein (MRP) and P-glycoprotein (Pgp) are both members of the superfamily of ATP binding cassette plasma membrane drug transport proteins, which may be partly responsible for multidrug resistance of tumor cells. Although MRP has been identified as an organic anion transporter and Pgp as a transporter of certain positively charged compounds, there is considerable overlap in resistance spectrum, suggesting that both proteins transport important anticancer agents such as doxorubicin, etoposide, and vincristine. To obtain more insight in the handling of drugs by both proteins, we performed a detailed kinetic analysis of the efflux of calcein−acetoxymethyl ester (CAL-AM), a common neutral substrate for both proteins and compared it with the kinetics of efflux of calcein (CAL) which is only effluxed by MRP. CAL, the hydrolysis product of the nonfluorescent CAL-AM, is negatively charged and highly fluorescent. For this purpose Pgp+ K562/ADR and MRP+ GLC4/ADR tumor cells were incubated with CAL-AM in ATP-rich or ATP-depleted buffer, and the calcein formation was followed in time by fluorescence development. The intracellular CAL could be distinguished from effluxed (extracellular) CAL by addition to the medium of Co^{2+}, which completely quenched the extracellular CAL fluorescence. The results showed that the V_{max} for efflux of CAL-AM and CAL by MRP were very similar ($1.0-1.2 \times 10^5$ molecules/cell/s) but that the K_m for CAL-AM was much lower (0.05 μM) than for CAL (268 μM). The latter therefore is much less efficiently transported by MRP than CAL-AM. The K_m for CAL-AM transport by Pgp (0.12 μM) was similar to that for MRP. Compared to previously published data for anthracyclines, the kinetic data for MRP-mediated CAL-AM pumping are most similar to those for the neutral hydroxydaunorubicin. These data give a quantitative account of transport properties of MRP for two related but differently charged compounds.

The *MRP*1-encoded multidrug resistance protein (MRP) and the *MDR*1 encoded P-glycoprotein (Pgp) are both plasma membrane transporters thought to be responsible in part for the resistance of tumor cells to multiple chemically unrelated drugs (MDR) (*1*−*3*). Both proteins belong to the superfamily of the so-called ATP binding cassette transport proteins or traffic ATPases (*4*), which are known to be dependent on ATP hydrolysis for the translocation of substrate across membranes. Both proteins have a broad substrate specificity which is only partly overlapping. MRP has been identified as a transporter of organic anions, such as leukotriene C_4 and dinitrophenyl glutathione (DNP-SG) (*5, 6*), whereas Pgp seems to prefer neutral or positively charged lipophilic molecules, such as rhodamine 123 or SYTO16 (*7, 8*). However, both proteins cause resistance to several important anticancer drugs, such as daunorubicin and doxorubicin, etoposide, and vincristine (*9, 10*), which suggests that these drugs belong to classes of overlapping substrates.

However, a clear distinction in the mechanism of translocation of these type of substrates by MRP or Pgp is indicated by the finding that their MRP-mediated transport is inhibited by depletion of intracellular glutathione (GSH), which has no effect on their Pgp-mediated transport (*11, 12*). For this reason it has been speculated that MRP would not transport the unmetabolized forms of these drugs, but only negatively charged metabolites, such as GSH-conjugates formed in the cells (*13*). Data from drug transport experiments using inside-out membrane vesicles prepared from MRP-overexpressing tumor cells have not yet been conclusive. Transport of unmodified drug (e.g. daunorubicin, *14*) as well as stimulation of the transport by GSH (for vincristine, *15*) has been reported. In addition it has been shown that the ATP-dependent transport of DNP-SG in inside-out vesicles from MRP-overexpressing cells can be inhibited among others by daunorubicin, etoposide, and vincristine (*16*). Taken together these data suggest that there may be overlapping binding-sites, where these different types of MRP substrates, such as exemplified by daunorubicin and the negatively charged DNP-SG may interact (*16*).

Little is known on the relative pumping efficiency by MRP of the different types of substrates. In the present study we have taken a kinetic approach to determine the relative

* Author to whom correspondence should be addressed. tel (33) 1 4838 7748. fax (33) 1 4838 7777. e-mail garnier@lpbc.jussieu.fr.
[‡] Université Paris Nord.
[§] Academisch Ziekenhuis Vrije Universiteit.

S0006-2960(97)01804-7 CCC: $15.00
Published on Web 02/04/1998

Chart 1

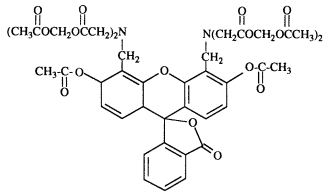

Calcein AM

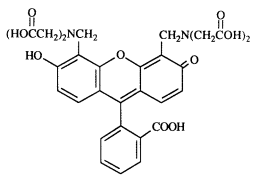

Calcein

pumping efficiency of two chemically related compounds, calcein acetoxymethyl ester (CAL-AM) and calcein (CAL) by MRP and Pgp. The neutral CAL-AM as well as its highly negatively charged hydrolysis product CAL (Chart 1) have both been identified as MRP substrates (*17*−*19*). In contrast only CAL-AM is a substrate for Pgp (*20*). Results from this study show that the V_{max} for CAL-AM and CAL transport by MRP is very similar, but that the apparent K_m for CAL is a factor 5000 higher than for CAL-AM.

MATERIALS AND METHODS

Cell Culture. K562 leukemia cells and the Pgp expressing K562/ADR cells (*21*), as well as GLC_4 and the MRP expressing cell line GLC_4/ADR (*22*) were cultured in RPMI 1640 (Sigma Chemical Co) medium supplemented with 10% fetal calf serum (Biomedia Co) at 37 °C in a humidified incubator at 5% CO_2. The GLC_4/ADR cells highly overexpress the *MRP*1 gene, but not the *MDR*1 (23) or the recently discovered *MRP*2,3,4 and 5 genes (*24*). The resistant K562/ADR and GLC_4/ADR cells were cultured with 400 nM and 1.2 μM doxorubicin, respectively. until one to three weeks before experiments. Cell cultures used for experiments were split 1:2 one day before use in order to ensure a logarithmic growth phase.

Drugs and Chemicals. Calcein acetoxy methyl ester was from Molecular Probes (Eugene, OR) and was dissolved in dimethyl sulfoxide as a stock solution of 1 mM and stored at −20 °C. According to the supplier, the lot of CAL-AM used has been determined by HPLC to be 91% pure. $CoCl_2$, analytical grade was from Aldrich and was dissolved in water. Triton X-100 and Digitonin (50% pure preparation) were from Sigma and were dissolved in water and used within 7 days. Before the experiments, the cells were counted, centrifuged, and resuspended in HEPES/Na buffer solutions containing 20 mM HEPES plus 132 mM NaCl, 3.5 mM KCl, 1 mM $CaCl_2$, and 0.5 mM $MgCl_2$, pH = 7.25 with or without 5 mM glucose.

Cellular Calcein Accumulation. The methodology for the determination of the kinetics of active transport of a drug from tumor cells has been extensively used and discussed before for the anthracyclines (*25*, *26*). We have now adapted this technique to measure the kinetics of active CAL-AM and CAL transport. Basically, the fluorescence signal is monitored continuously during incubation of the cells with CAL-AM or the efflux of CAL from the cells. Since CAL-AM itself is a nonfluorescent molecule, the fluorescence that is measured is always that of the CAL, which is formed inside the cells by cytoplasmic esterases. To distinguish intra- from extracellular CAL, 2 μM Co^{2+} is added to the cells, which completely quenches the extracellular CAL fluorescence. This concentration of Co^{2+} has been selected in preliminary experiments and was not toxic to the cells during the experiments.

The cells are always incubated in a quartz cuvette in a suspension of 10^6 cells/mL in HEPES buffer with/without 10 mM sodium azide and 5 mM glucose as indicated. The fluorescence is recorded on a Perkin-Elmer LS50B spectrofluorometer at 515 nm (λ_{ex} = 493 nm). A preincubation with azide in glucose-free buffer is used in some of the experiments to deplete cellular ATP, which blocks the active drug efflux. Then cells are incubated with CAL-AM until a plateau is reached. This method has been extensively tested and validated for the measurement of efflux kinetics of anthracyclines using these cell lines (*25*−*28*). Details of the experimental setups are given in the Results section.

Mathematical Calculations. The maximal efflux rates (V_{max}), apparent Michaelis−Menten constants (K_m), and cooperativity constants (n_H) for the transport of CAL-AM and CAL were computed by nonlinear regression analysis of transport velocity (V_a) versus free intracellular CAL-AM or CAL concentration (C_i = $[CAL\text{-}AM]_i$ or $[CAL]_i$) data using the MacCurveFit program and assuming that the transport follows the Hill equation (*29*):

$$V_a = V_{max} C_i^{nH} / (K_m^{nH} + C_i^{nH}) \quad (1)$$

RESULTS

Establishment of the Experimental Model. To be able to calculate the kinetic parameters for the active transport of the substrates CAL-AM and CAL, we have performed a series of experiments designed to determine the relationship between the extracellular or outside ($[CAL\text{-}AM]_o$) and intracellular ($[CAL\text{-}AM]_i$ and $[CAL]_i$) concentrations. The principle of these experiments is shown in Figure 1 for K562 and in Figure 2 for GLC_4 cells, where typical curves of individual experiments are shown. Cell samples were preincubated with azide in glucose-free buffer for 30 min (− energy) or cells were incubated in buffer with glucose (+ energy). Then the cells were incubated with CAL-AM in a range of concentrations (0.025−5 μM) with or without 2 μM Co^{2+}, and the development of fluorescence was monitored in all these situations until a pseudo steady-state (F_{ss}) was reached (see later).

The fluorescence which develops represents the formation of CAL from CAL-AM by cytoplasmic esterases. This reaction is not ATP-dependent, since in the sensitive cells (i.e. cells without active drug efflux) we did not see any difference in CAL formation in ATP-depleted versus ATP rich cells (Figure 1A for K562 and Figure 2A for GLC_4). Thus the difference in fluorescence development (or CAL formation) between ATP depleted (dF_3/dt) and ATP-rich cells (dF_1/dt) is caused by the ATP-dependent efflux of CAL-AM and therefore:

$$d[CAL\text{-}AM]/dt = (dF_3/dt - dF_1/dt)[CAL\text{-}AM]_{o,t=0}/F_{ss} \quad (2)$$

at any time point represents the rate of CAL-AM transport out of the cells at that time (see Figure 1B for K562/ADR and Figure 2B for GLC_4/ADR).

Subsequently, when F_{ss} is reached the ATP-depleted cells can be used to measure the ATP-dependent CAL efflux by adding glucose, which restores the glycolytic ATP synthesis

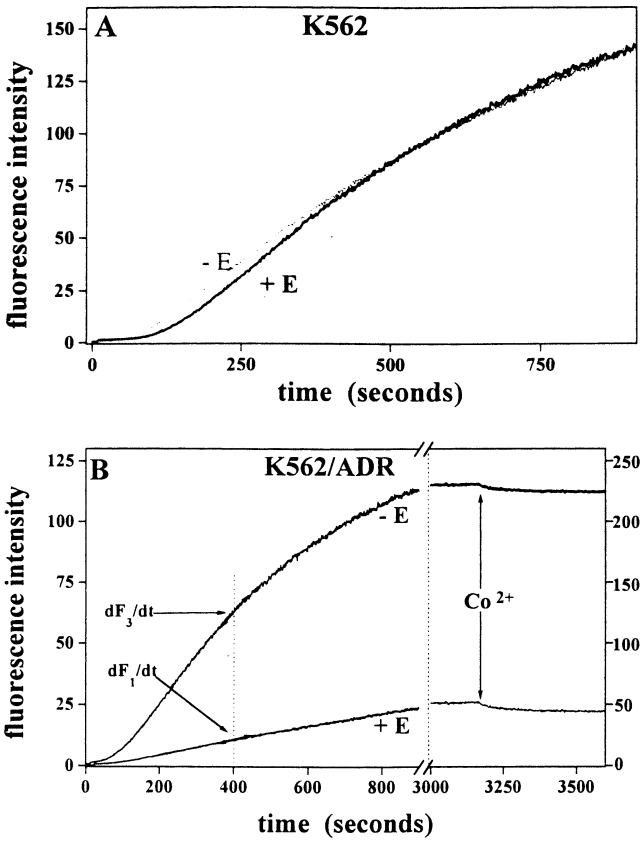

FIGURE 1: Fluorescence recordings at 515 nm of ATP-rich (+E) and ATP-depleted (−E) K562 (A) and K562/ADR (B) cells incubated with 1 μM $[CAL\text{-}AM]_{0,t=0}$. Where indicated 2 μM Co^{2+} has been added.

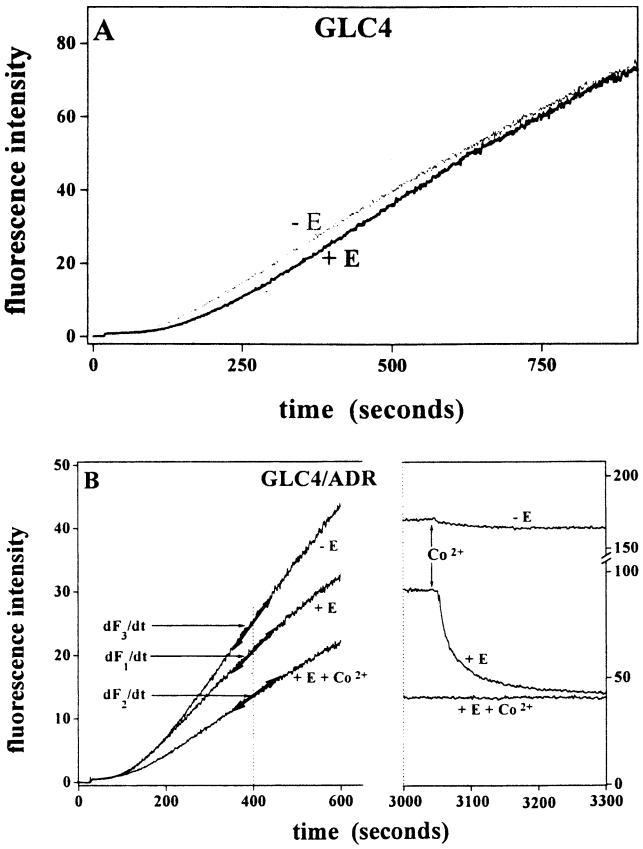

FIGURE 2: Fluorescence recordings at 515 nm of ATP-rich (+E) and ATP-depleted (−E) GLC_4 (A) and GLC_4/ADR (B) cells incubated with 1 μM $[CAL\text{-}AM]_{0,t=0}$. Where indicated 2 μM Co^{2+} has been added.

(*25*, *26*, *28*). In all experiments, in which we wish to determine directly or indirectly the CAL efflux from the cells, the use of Co^{2+} is an important tool because it quenches the extracellular CAL fluorescence. This allows us to record only the CAL that remains inside the cells and thus the kinetics of CAL transport across the plasma membranes. Examples of recordings with Co^{2+} are given in the Figures 1−3. Figure 3 shows that Co^{2+} does not cause quenching of the CAL fluorescence in the Pgp-overexpressing K562/ADR cells, confirming the specificity of this approach to show MRP-mediated CAL efflux. We have checked that Co^{2+} had no effect on CAL fluorescence when added to the parental cell lines during their incubation with CAL-AM.

Control Experiments. After having established the principle of the experiments as explained above, a set of control experiments was performed in order to further validate the use of the experimental model to analyze the transport kinetics of CAL-AM and CAL.

First, the recordings of CAL formation in time in all cells had the form as shown in the examples of Figures 1 and 2, appearing as a sigmoid curve until a plateau (F_{ss}) was reached in about 1 h. In the next 30 min. a further increase of maximal 2% of the F after 1 h occurred. The relation of F_{ss} with initial $[CAL\text{-}AM]_o$ is depicted in Figure 4 for the GLC_4/ADR cells depleted of energy. A similar curve was obtained for the K562/ADR cells (not shown). The curve was linear up to 2 μM $[CAL\text{-}AM]_{o,t=0}$. After 60 min incubation of ATP-depleted GLC_4/ADR cells we have added 2 μM Co^{2+}, after which no or a very minor decrease of fluorescence signal was seen (Figure 2B). This shows that the ATP

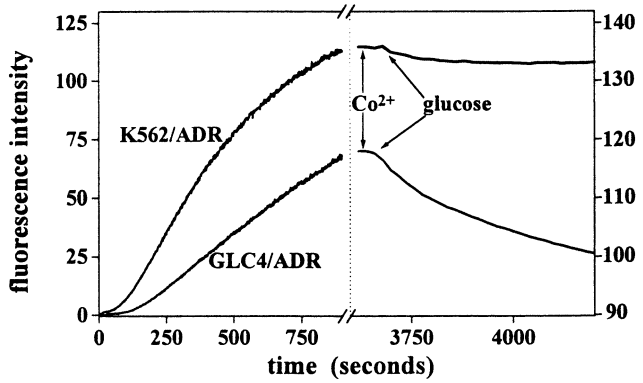

FIGURE 3: ATP-depleted GLC_4/ADR or K562/ADR cells were incubated with 1 μM $[CAL\text{-}AM]_{o,t=0}$ and at F_{ss} 2 μM Co^{2+} was added. Then 5 mM glucose was added to restore ATP synthesis. Only in the case of MRP-overexpressing cells GLC_4/ADR cells quenching of (effluxed) CAL is seen.

depletion was sufficient to block the ATP-dependent CAL efflux during the CAL-AM loading period. We have checked that during the 60 min in solution the degradation of CAL-AM was less than 1%.

A second control experiment was done in order to establish that the fluorescence properties of CAL under these conditions are the same inside or outside the cells. Therefore at the F_{ss} we permeabilized the plasma membranes with 0.01% Triton X-100 and we found up to an initial loading $[CAL\text{-}AM]_o$ of 2 μM an increase of 10% at most of F_{ss} (which at this point was quenched for more than 95% by 2 μM Co^{2+}). This indicates that there are only minor differences in CAL

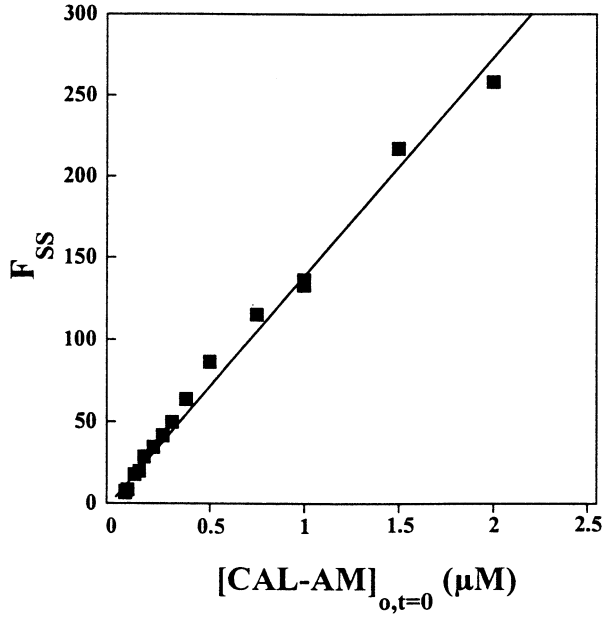

FIGURE 4: Pseudo-steady-state fluorescence (F_{ss}), after incubation of ATP-depleted GLC_4/ADR cells for 60 min with different initial concentrations of CAL-AM. A linear relationship of F_{ss} with concentration was found up to 2 μM $[CAL\text{-}AM]_{o,t=0}$.

fluorescence in- or outside the cells and that there does not seem to be self-quenching of CAL *at* the high $[CAL]_i$ which are reached in the intracellular volume (see later). In addition we examined the GLC_4/ADR cells by fluorescence microscopy after loading with CAL-AM. It appeared that in these cells the CAL fluorescence was evenly distributed throughout the nucleus and cytoplasm when ATP-depleted cells were used. In ATP-rich cells, CAL was partly present in a punctate-like cytoplasmic compartment, with a somewhat higher fluorescence than the main cytoplasm. Together these results justify the assumption that for our calculations the CAL may be regarded as evenly distributed without evidence of self-quenching up to 2 μM $[CAL\text{-}AM]_{o,t=0}$.

In a third control experiment cells that had been incubated for 1 h with an initial loading concentration of 1 or 2 μM CAL-AM were centrifuged and to the supernatant fresh cells were added. Upon incubation of those cells no fluorescence developed, showing that at F_{ss} virtually all CAL-AM had been taken up by the cells and was converted into CAL. Therefore we can calculate $[CAL]_i$ from $[CAL\text{-}AM]_{o,t=0}$.

A fourth control experiment was done, because for the complete analysis of CAL-AM kinetics we also need to know the intracellular CAL-AM concentration ($[CAL\text{-}AM]_{i,t}$) at any time during the incubations. To know these concentrations we have to know whether the passage of CAL-AM through the plasma membranes or the kinetics of the esterase reaction is the rate-limiting step in the process leading to CAL formation. Therefore we applied a mild permeabilization of the K562 cells with increasing concentrations of digitonin and coincubated the cells with CAL-AM. Under these conditions, no increase of the rate of CAL formation was seen, indicating that the esterase reaction and not the membrane passage of CAL-AM was rate-limiting. The decrease of CAL formation was seen at digitonin concentrations above 5 μM probably caused by leakage of esterase from the cells. As a control for plasma membrane permeabilization by digitonin we measured the uptake of doxorubicin under the same conditions according to previously published methods (*21*, *25*). The entry of the anthracycline doxorubicin which has slow cellular uptake kinetics was clearly shown to be facilitated at digitonin concentrations of 3−4 μM. Another substrate tested was a tetramethylrhodamine labeled 20 base-pair containing oligonucleotide, which entered the cell at the same digitonin concentration as doxorubicin (not shown). From these data we conclude that after permeabilization of the cellular plasma membranes for small MW molecules no increase of $[CAL\text{-}AM]_i$ occurs in these sensitive cells, apparently because their is a rapid repartition of CAL-AM over the cell membrane, which obeys to transmembrane equilibrium.

A fifth control experiment was done to check the ATP intracellular level under the different experimental conditions. The ATP concentration was determined using the luciferin−luciferase test. In both cell lines the ATP concentration was 2.5 ± 0.5 mM. The presence of azide under glucose-free conditions yielded 90% ATP depletion. The subsequent addition of glucose bring ATP levels back to control value within about 2 min.

Based on these control experiments, the following results and discussion is based on data obtained by incubation of cells with ≤ 2 μM $[CAL\text{-}AM]_{o,t=0}$. Under these conditions the fluorescence signal is proportional to [CAL], whether it is intra- or extracellularly localized. Furthermore, $[CAL]_i$ and $[CAL\text{-}AM]_i$ can be derived from $[CAL\text{-}AM]_o$ at any time of the incubations. These calculations will be presented below.

Kinetics of Calcein Formation in ATP-Depleted GLC_4/ADR and K562/ADR Cells. From the F_{ss} measured after incubation of the resistant cells in ATP-depleted conditions with 0.05−2 μM $[CAL\text{-}AM]_{o,t=0}$ the kinetics of CAL formation are calculated as a function of $[CAL\text{-}AM]_i$ which under these conditions is equal to $[CAL\text{-}AM]_o$, as discussed before. This was done by taking the slope of the tangent of the curves of F_3 at 400 s, recorded at 0.05−2 μM $[CAL\text{-}AM]_{o,t=0}$, as shown in Figures 1 and 2.

Now $d[CAL]/dt$ and $[CAL\text{-}AM]_{o,t}$ at time t follow from:

$$\frac{d[CAL]}{dt} = \left(\frac{[CAL\text{-}AM]_{o,t=0}}{F_{ss}}\right)\frac{dF_3}{dt} \tag{3}$$

$$[CAL\text{-}AM]_{o,t} = [CAL\text{-}AM]_{o,t=0} - \left(\frac{F_3}{F_{ss}}\right)[CAL\text{-}AM]_{o,t=0} \tag{4}$$

If we assume that the esterase reaction follows Hill kinetics (eq 1), the data can be fitted by nonlinear regression. The results are shown in Figure 5 for GLC_4/ADR cells and in Figure 6 for K562/ADR cells. Thus using these figures as calibration and the equations A and B, which follow from them (see the legends of these figures), we are now able to calculate the intracellular CAL-AM concentration ($[CAL\text{-}AM]_i$) in any condition from the kinetics of CAL formation. In particular, these equations will be used later to calculate the $[CAL\text{-}AM]_i$ from the kinetics of fluorescence appearance in ATP-rich cells.

Kinetics of Pgp-Mediated CAL-AM Efflux from K562/ADR Cells. K562/ADR cells (10^6/mL) were incubated with 0.05−2 μM $[CAL\text{-}AM]_{o,t=0}$ in glucose- or azide-containing

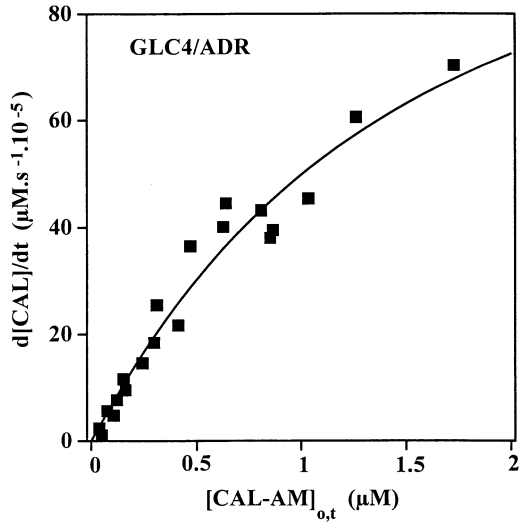

FIGURE 5: The rate of calcein formation d[CAL]/dt (μM/s $\times$ 10^{-5}) in ATP-depleted GLC_4/ADR cells determined from the tangent to the slope at 400 s of the curves (as shown in Figure 2) for loading with 0.05−2 μM $[CAL\text{-}AM]_{o,t=0}$. The parameters V_{max} (126 ± 50 $\times$ 10^{-5} μM s^{-1}), K_m (1.5 ± 1 μM) and n_H (1 ± 0.2) as found by nonlinear fit can be put into the equation A: $d[CAL]/dt = 126 \times 10^{-5}[CAL\text{-}AM]_i/1.5 + [CAL\text{-}AM]_i$.

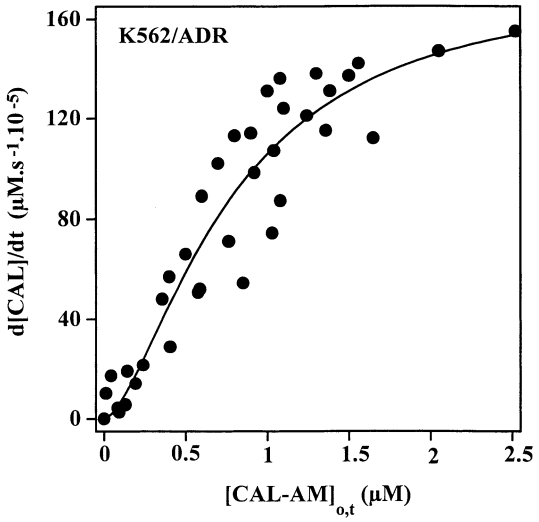

FIGURE 6: The rate of calcein formation d[CAL]/dt (μM/s $\times$ 10^{-5}) in ATP-depleted K562/ADR cells determined from the tangent to the slope at 400 s of the curves (as shown in Figure 1) for loading with 0.05−2 μM $[CAL\text{-}AM]_{o,t=0}$. The parameters V_{max} (180 ± 30 $\times$ 10^{-5} μM s^{-1}), K_m (0.8 ± 0.2 μM) and n_H (1.6 ± 0.3) as found by nonlinear fit can be put into the equation B: $d[CAL]/dt = 180 \times 10^{-5}[CAL\text{-}AM]_i^{1.6}/(1.5)^{1.6} + [CAL\text{-}AM]_i^{1.6}$.

buffer, and the fluorescence was recorded in time. Representative curves were shown in Figure 1B. As expected, the CAL formation in ATP-rich Pgp expressing cells at any $[CAL\text{-}AM]_{o,t=0}$ was less than in ATP-depleted cells, due to Pgp-mediated CAL-AM efflux. If Co^{2+} was added, no or a very minor effect was seen. Again, the kinetics of CAL formation under these conditions was determined from the tangent to the slopes of the curves at t = 400 s and plotted as a function of $[CAL\text{-}AM]_{o,t=400}$ (Figure 7). $[CAL\text{-}AM]_i$ is now calculated from the d[CAL]/dt for every data point, using equation B as discussed before.

Thus the rate of active efflux of CAL-AM (V_a) as a function of $[CAL\text{-}AM]_i$ can now be calculated from Figure 6 (equation B) and Figure 7 and is plotted in Figure 8. The

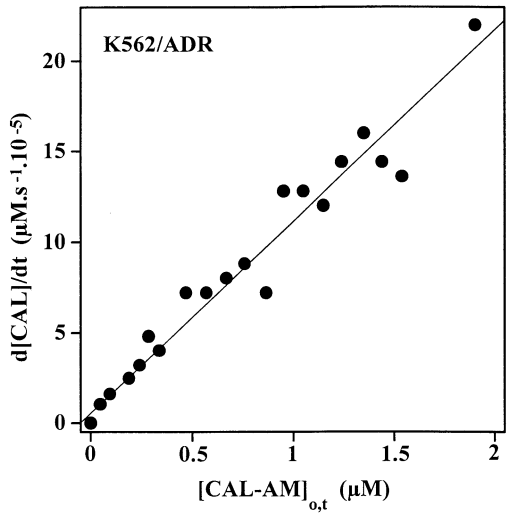

FIGURE 7: The rate of calcein formation d[CAL]/dt (μM/s x 10^{-5}) in ATP-rich K562/ADR cells as a function of $[CAL\text{-}AM]_{o,t}$ determined from the tangent to the slope at 400 s of the curves (as shown in Figure 1) for loading with 0.05−2 μM $[CAL\text{-}AM]_{o,t=0}$.

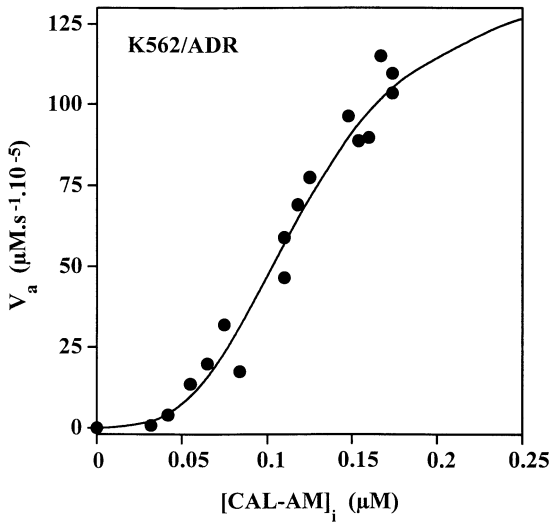

FIGURE 8: Rate of ATP-dependent CAL-AM efflux (V_a) by K562/ADR cells as a function of $[CAL\text{-}AM]_i$, determined from the difference between the slopes at 400 s of the fluorescence recordings curves of ATP-depleted and ATP-rich cells using 0.05−2 μM $[CAL\text{-}AM]_{o,t=0}$.

kinetic parameters from the nonlinear fit based on Hill kinetics are shown in Table 1.

Kinetics of MRP-Mediated CAL-AM Efflux from GLC_4/ADR Cells. GLC_4/ADR cells (10^6/mL) were incubated with 0.05−2 μM $[CAL\text{-}AM]_{o,t=0}$ in glucose- or azide-containing buffer, and the fluorescence was recorded in time. Representative curves were shown in Figure 2B. The parameters for the MRP-mediated CAL-AM efflux are determined exactly as was done for Pgp-mediated CAL-AM efflux. This can be done despite the fact that in ATP-rich conditions (glucose addition) CAL will be effluxed together with CAL-AM, because the CAL fluorescence is the same whether it remains inside the cells or is effluxed by MRP (see second control experiment). Figure 9 shows the rate of CAL formation as determined from the tangent to the slopes of the curves at t = 400 s and plotted as a function of $[CAL\text{-}AM]_{o,t=400}$. The curves for the active efflux rate (V_a) of CAL-AM as a function of $[CAL\text{-}AM]_i$ can now be calculated from Figure 5 (equation A) and Figure 9 and is plotted in Figure

Table 1: Summary of the Kinetic Parameters of Active CAL-AM and CAL Efflux[a]

	Pgp CAL-AM	Pgp daunorubicin	Pgp OH-Dauno	MRP CAL	MRP CAL-AM	MRP daunorubicin	MRP OH-Dauno
V_{max} (nM s^{-1})	1.4 ± 0.1	3.4 ± 0.3	2.6 ± 0.6	0.17 ± 0.04	0.20 ± 0.01	2.0 ± 0.2	0.26 ± 0.04
K_m (μM)	0.12 ± 0.01	2.1 ± 0.3	2.4 ± 0.7	268 ± 160	0.05 ± 0.01	0.8 ± 0.2	0.6 ± 0.1
n_H	3.2 ± 0.5	1.9 ± 0.4	1.8 ± 0.6	1.0 ± 0.2	1.3 ± 0.3	1.8 ± 0.5	1.9 ± 0.8
$k_a \times 10^{10}$ s^{-1} (cell/mL)$^{-1}$	63	8	5	2.2×10^{-3}	23	13	2

[a] Data for CAL and CAL-AM are from this study. Data for daunorubicin and hydroxydaunorubicin (OH-Dauno) obtained with the same cell lines are from ref 28 and are shown for comparison. The $k_a = 1/n(V_{max}/n_H K_m)\,(n_H - 1)^{(1 - 1/n_H)}$, in which n is the number of cells/mL, is the slope of the tangent to the curve $V_a = f$[substrate] when [substrate] $= K_m(n_H - 1)^{(1 - 1/n_H)}$ and has been defined in that paper. The parameter k_a allows a convenient comparison of the transport efficiency of different substrates in the same cells.

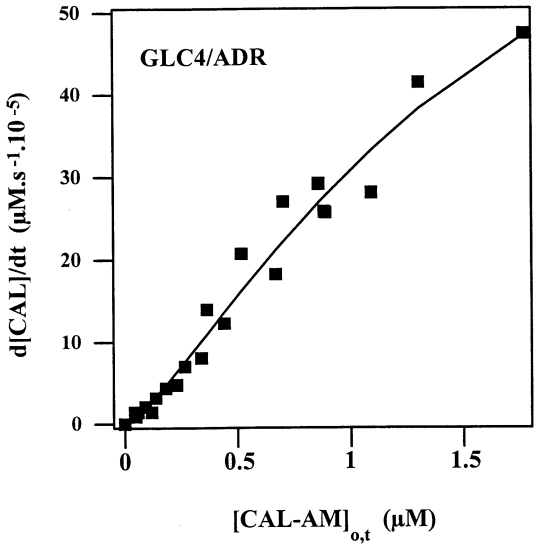

FIGURE 9: The rate of calcein formation d[CAL]/dt (μM/s x 10^{-5}) in ATP-rich GLC_4/ADR cells as a function of $[CAL\text{-}AM]_{o,t}$ determined from the tangent to the slope at 400 s of the curves (as shown in Figure 2) for loading with 0.05−2 μM $[CAL\text{-}AM]_{o,t=0}$.

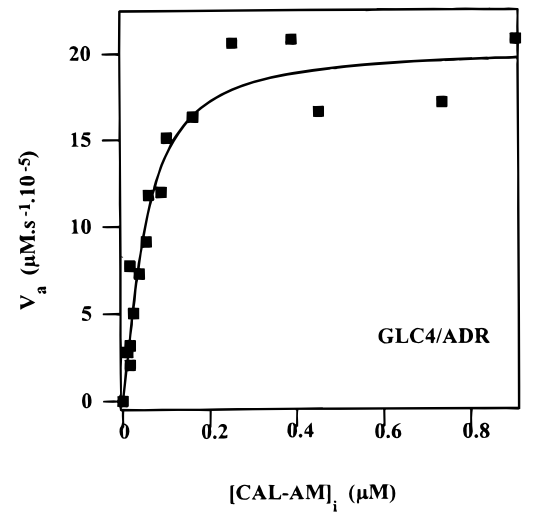

FIGURE 10: Rate of ATP-dependent CAL-AM (V_a) efflux by GLC_4/ADR cells as a function of $[CAL\text{-}AM]_i$, determined from the difference between the slopes at 400 s of the fluorescence recordings curves of ATP-depleted and ATP-rich cells using 0.05−2 μM $[CAL\text{-}AM]_{o,t=0}$.

10. The kinetic parameters from the nonlinear fit based on Hill kinetics are shown in Table 1.

Kinetics of MRP-Mediated Calcein Efflux from GLC$_4$/ADR Cells. The kinetics of CAL efflux from the GLC_4/ADR cells was determined from the difference in fluorescence between the recordings in glucose-containing buffer in the presence

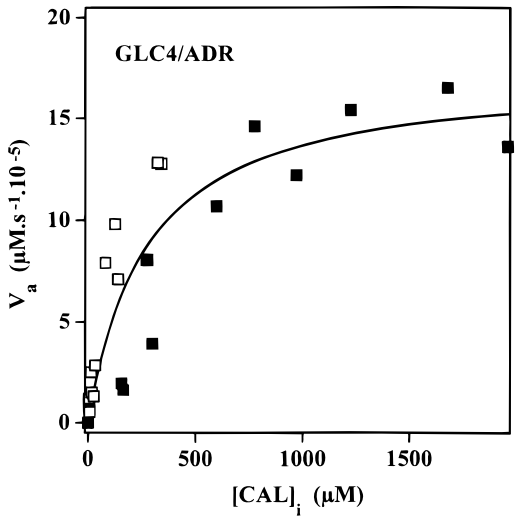

FIGURE 11: The active CAL efflux rate (V_a) from GLC_4/ADR cells as a function of $[CAL]_i$.Data points are from two differents methods as described in detail in results: method 1 (□) is based on subtraction of CAL formation rates ($dF_1/dt - dF_2/dt$ as in Figure 2B) Method 2 (■) is a direct efflux measurement as illustrated in Figure 3.

or absence of 2 μM Co^{2+}: $(d[CAL]/dt)_1 - (d[CAL]/dt)_2$ in Figure 2B. The $[CAL]_i$ can be calculated from the F_{ss} because all the known amount of added CAL-AM is then converted into CAL as discussed before. For the cellular volume a value of 10^{-12} L was taken. Because of a little impurity in the lot of CAL-AM, which was 91% pure according to the supplier, and because the volume of the cells was an estimation, the estimation of the absolute $[CAL]_i$ will reflect these uncertainties.

A second method was used to directly determine the kinetics of MRP-mediated CAL efflux. ATP-depleted GLC_4/ADR cells were incubated with 0.05−2 μM $[CAL\text{-}AM]_{o,t=0}$ for 1 h. Then when F_{ss} is reached, 2 μM Co^{2+} was added and then glucose to restore ATP synthesis and ATP-dependent CAL efflux. A typical example of such an experiment was given in Figure 3. The kinetics of d[CAL]/dt can now be determined directly from the slope of these curves recorded with different $[CAL\text{-}AM]_{o,t=0}$. Again $[CAL]_i$ is calculated from F_{ss} at the time of addition of glucose. The results of both determinations of the active CAL efflux (V_a) are depicted in Figure 11. The analysis of the data obtained using method 1 yielded $V_{max} = 0.18 \pm 0.05$ n M s^{-1}, $K_m = 150 \pm 90$ μM, $n_H = 1.3 \pm 0.2$. The analysis of the data obtained using method 2 yielded $V_{max} = 0.15 \pm 0.02$ nM s^{-1}, $K_m = 370 \pm 70$ μM, $n_H = 2.1 \pm 0.6$. The agreement between the values obtained by both methods was quite good for V_{max} but somewhat less for the K_m which is reflected in

the large SD for the K_m as obtained by analysis of the whole data set as shown in Table 1.

DISCUSSION

This study provides a kinetic analysis of the ATP-dependent efflux of CAL-AM and CAL from tumor cells, mediated by two different plasma membrane drug transporter proteins, MRP and Pgp.

Previous studies have shown that the nonfluorescent CAL-AM was actively protected from hydrolysis by the cytosolic esterases in tumor cells which overexpress Pgp (*20*). The result from that study was actually considered by the authors as evidence in support of the vacuum cleaner hypothesis for the action of Pgp, first proposed by others (*30*). In the vacuum cleaner model the hydrophobic substrate molecules will enter the membrane lipid bilayer from outside the cell following their concentration gradient and will then be extracted directly from the membrane bilayer by Pgp and extruded back to the extracellular medium. In this concept the cytoplasmic esterases will never *see* the pumped CAL-AM molecules and therefore will have no chance to hydrolyze them.

In that study of Homolya et al. (*20*) as well as in our present analysis it was essential to determine the rate-limiting step in this process, the plasma membrane passage of CAL-AM or the cytosolic CAL-AM hydrolysis to the fluorescent CAL, which is the actually measured species. Our data showed that gentle opening of the plasma membrane of K562 cells for small (doxorubicin) to medium sized (20 base pair oligonucleotides) molecules did not lead to an increase of CAL formation of these cells upon incubation with CAL-AM. This can only be explained by the fact that CAL-AM is equilibrating very rapidly over the cellular plasma membrane resulting in the same in- and outside concentrations of CAL-AM rapidly after the start of the incubations.

Therefore, since apparently the esterase reaction is rate-limiting for CAL formation, we conclude that this type of data cannot be used as support for the vacuum cleaner model of pump action. On the other hand, for our kinetic analysis, this finding allowed us to take the $[CAL\text{-}AM]_{i,t}$ equal to $[CAL\text{-}AM]_{o,t}$ at any time t during the incubations, where there is no active efflux (sensitive cells or ATP-depleted resistant cells).

From the summary of the presently found kinetic parameters (see Table 1) it can be seen that the charged CAL (the net charge is 4^-) and the neutral substrate CAL-AM have a very similar V_{max} in GLC_4/ADR cells, both of about 0.2 nM s^{-1} or 1×10^5 molecules/cell/s pumped out. However, the K_m for transport of the neutral CAL-AM was about a factor 5000 lower than for the negatively charged CAL. Still there is appreciable transport of CAL from MRP-overexpressing cells, since the $[CAL]_i$ is in the mM range. A lower K_m for CAL-AM is in accordance with a stronger (30-fold) inhibition of dinitrophenyl glutathione transport compared to CAL in inside-out vesicles prepared from GLC_4/ADR cells as reported recently (*16*). It may be remarkable that the affinity of MRP for the negatively charged species CAL is so much lower than for the neutral CAL-AM, whereas the substrate specificity of MRP with respect to organic anions resembles that of the multiple organic anion transporter (MOAT) (*5, 6, 31*). On the other hand, there is evidence for the transport by MRP of such different compounds as estradiol-glucuronides (*32*) or glucuronosyl-etoposide (*33*) as well as not (negatively) charged compounds, such as daunorubicin and etoposide (*34*). Also, competitive inhibition of the latter transport by the not charged genistein has been reported (*35*).

If we compare the kinetic parameters for the transport by MRP of CAL-AM and CAL with the anthracyclines daunorubicin and hydroxydaunorubicin (see Table 1), then it can be seen that the V_{max} for daunorubicin is 10 times higher (order of 10^6 molecules/cell/s) than for both CAL-AM and CAL, whereas the uncharged hydroxydaunorubicin (which has OH instead of the protonatable amino group) has a V_{max} comparable to CAL and CAL-AM. The parameter k_a, which is proportional to V_{max}/K_m allows an easy comparison of the transport efficiency of the various substrates. Again, the low efficiency of CAL as MRP substrate compared to the anthracyclines can be seen. It remains to be studied whether the high negative charge of CAL (net charge -4 at pH $=$ 7.0) precludes it to be a highly efficient MRP substrate.

A remark which can be made with respect to the comparison of CAL-AM with highly lipophilic anthracyclines such as idarubicin is that, despite the rapid membrane passage of CAL-AM, the MRP and Pgp pump activity for CAL-AM is apparently high enough to account for a considerable decrease in intracellular concentration. For highly lipophilic anthracyclines, however, the accumulation defect as well as the resistance in MRP or Pgp overexpressing cells is almost or completely absent, due to the fact the pump capacity is not high enough to cope with a high passive influx (*21, 27, 36*). This is probably related to the low apparent K_m for CAL-AM of MRP and Pgp, which is a factor 10−20 lower than for most anthracyclines.

In conclusion, this study present kinetic data for the transport of two chemically related compounds, CAL-AM and its hydrolysis product CAL, which are neutral and negatively charged substrates for MRP. CAL appeared to be transported much less efficiently than CAL-AM. The V_{max} of CAL-AM transport by MRP or Pgp appeared to be very similar to those values for the neutral anthracycline hydroxydaunorubicin. Compared to CAL-AM and hydroxydaunorubicin, the protonatable group in daunorubicin seems important for an enhanced pumping rate by Pgp (*37*) as well as MRP. These quantitative data on transport kinetics of MRP further our insight into the chemical requirements of molecules in order to be recognized as substrates and effluxed by MRP. These data may direct research toward ways to selectively interfere with the substrate transport and ultimately in the design of drugs to improve cancer therapy.

ACKNOWLEDGMENT

This study was supported by the Centre National de la Recherche Scientifique and the Université Paris Nord. We thank Patricia Quidu for her technical assistance and Frédéric Frézard for useful discussions.

REFERENCES

1. Cole, S. P. C., Bhardwaj, G., Gerlach, J. H., Mackie, J. E., Grant, C. E., Almquist, K. C., Stewart, A. J., Kurz, E. U., Duncan, A. M. V., and Deeley, R. G. (1992) *Science 258*, 1650−1654.
2. Bradley, G., Juranka, P. F., and Ling, V. (1988) *Biochem. Biophys. Acta 948*, 87−128.

3. Broxterman, H. J., Giaccone, G., and Lankelma, J. (1995) *Curr. Opinion Oncol. 7*, 532−540.
4. Higgins, C. F. (1992) *Annu. Rev. Cell Biol. 8*, 67−113.
5. Leier, I., Jedlitschky, G., Buchholz, U., Cole, S. P. C., Deeley, R. G., and Keppler, D. (1994) *J. Biol. Chem. 269*, 27807−27810.
6. Müller, M., Meijer, C., Zaman, G. J. R., Borst, P., Scheper, R. J., Mulder, N. H., de Vries, E. G. E., and Jansen, P. L. M. (1994) *Proc. Natl. Acad. Sci. USA 91*, 13033−13037.
7. Lampidis, T. J., Munck, J. N., Krishan, A., and Tapiero, H. (1985) *Cancer Res. 45*, 2626−2631.
8. Broxterman, H. J., Schuurhuis, G. J., Lankelma, J., Oberink, J. W., Eekman, C. A., Claessen, A. M. E., Hoekman, K., Poot, M., and Pinedo, H. M. (1997) *Br. J. Cancer 76*, 1029−1034.
9. Grant, C. E., Valdimarsson, G., Hipfner, D. R., Almquist, K. C., Cole, S. P. C., and Deeley, R. G. (1994) *Cancer Res. 54*, 357−361.
10. Zaman, G. J. R., Flens, M. J., van Leusden, M. R., de Haas, M., Mülder, H. S., Lankelma, J., Pinedo, H. M., Scheper, R. J., Baas, F., Broxterman, H. J., and Borst, P. (1994) *Proc. Natl. Acad. Sci. U.S.A. 91*, 8822−8826.
11. Davey, R. A., Longhurst, T. J., Davey, M. W., Belov, L., Harvie, R. M., Hancox, D., and Wheeler, H. (1995) *Leuk. Res. 19*, 275−282.
12. Versantvoort, C. H. M., Broxterman, H. J., Bagrij, T., Scheper, R. J., and Twentyman, P. (1995) *Br. J. Cancer 72*, 82−89.
13. Ishikawa, T., Akimaru, K., Tien Kuo, M., Priebe, W., and Suzuki, M. (1995) *J. Natl. Cancer Inst. 87*, 1639−1640.
14. Paul, S., Breuninger, L. M., and Kruh, G. D. (1996) *Biochemistry 35*, 14003−14011.
15. Loe, D. W., Almquist, K. C., Deeley, R. G., and Cole, S. P. C. (1996b) *J. Biol. Chem. 271*, 9675−9682.
16. Heijn,M., Hooijberg, J. H., Scheffer, G. L., Szabó, G., Westerhoff, H. V., and Lankelma, J. (1997) *Biochem. Biophys. Acta 1326*, 12−22.
17. Feller, N., Kuiper, C. M., Lankelma, J., Ruhdal, J. K., Scheper, R. J., Pinedo, H. M., and Broxterman, H. J. (1995) *Br. J. Cancer 72*, 543−549.
18. Feller, N. Broxterman, H. J., Währer, D. C. R., and Pinedo, H. M. (1995) *FEBS Lett. 308*, 385−388.
19. Holló, Z., Homolya, L, Hegedüs, T., and Sarkadi, B.(1996) *FEBS Lett. 383*, 99−104.
20. Homolya, L., Holló, Z., Germann, U. A., Pastan, I., Gottesman, M. M., and Sarkadi, B. (1993) *J. Biol. Chem. 268*, 21493−21496.
21. Mankhetkorn, S., Dubru, F., Hesschenbroek, M., Fiallo, M., and Garnier-Suillerot, A. (1996) *Mol. Pharmacol. 49*, 532−539.
22. Zijlstra, J. G., de Vries, E. G. E., and Mulder, N. H. (1987) *Cancer Res. 47*, 1780−1784.
23. Versantvoort, C. H. M., Broxterman, H. J., Pinedo, H. M., de Vries, E. G. E., Feller, N., Kuiper, C. M., and Lankelma, J. (1992) *Cancer Res. 47*, 17−23.
24. Kool, M., de Haas, M., Scheffer, G. L., Scheper, R. J., van Eijk, M. J. T., Juijn, J. A., Baas, F., and Borst, P. (1997) *Cancer Res. 57*, 3537−3547.
25. Frézard, F., and Garnier-Suillerot, A. (1991) *Biochim. Biophys. Acta 1091*, 29−35.
26. Frézard, F., and Garnier-Suillerot, A. (1991) *Eur. J. Biochem. 196*, 483−491.
27. Garnier-Suillerot, A. (1995). *Curr. Pharmaceut. Des. 1*, 69−82.
28. Marbeuf-Gueye, C., Broxterman, H. J., Dubru, F., Priebe, W., and Garnier-Suillerot, A. (1997) *Mol. Pharmacol.* (in press).
29. Hill, T. (1985) *Cooperative Theory in Biochemistry*, pp 63−67, Springer-Verlag, Berlin.
30. Raviv, Y., Pollard, H. B., Bruggemann, E. P., Pastan, I., and Gottesman, M. M. (1990) *J. Biol. Chem. 265*, 3975−3980.
31. Oude Elferink, R. P. J., Ottenhoff, R., Radominska, R., Hofmann, A. F., Kuipers, F., and Jansen, P. L. M. *Biochem. J. 274*, 281−286.
32. Loe, D. W., Almquist, K. C., Cole, S. P. C., and Deeley, R. G. (1996) *J. Biol. Chem. 271*, 9683−9689.
33. Jedlitschky, G., Leier, I., Buchholz, U., Barnouin, K., Kurz, G., and Keppler, D. (1996) *Cancer Res. 56*, 988−994.
34. Broxterman, H. J., Heijn, M., and Lankelma, J. (1996) *J. Natl. Cancer Inst. 88*, 466−467.
35. Versantvoort, C. H. M., Broxterman, H. J., Lankelma, J., Feller, N., and Pinedo, H. M. (1994) *Biochem. Pharmacol. 48*, 1129−1136.
36. Stein, W. (1997) *Physiol. Rev. 77*, 545−590.36. Stein, W. (1997) *Physiol. Rev. 77*, 545−590.
37. Lampidis, T. J., Kolonias, D., Podona, T., Israel, M., Safa, A. R., Lothstein, L., Savaraj, N., Tapiero, H., and Priebe, W. (1997) *Biochemistry 36*, 2679−2685.

BI9718043